



JAK3 inhibitors based on thieno[3,2-*d*]pyrimidine scaffold: design, synthesis and bioactivity evaluation for the treatment of B-cell lymphoma

Fuyun Chi^{a,1}, Lixue Chen^{a,b,1}, Changyuan Wang^a, Lei Li^a, Xiuli Sun^c, Youjun Xu^b, Tengyue Ma^d, Kexin Liu^a, Xiaodong Ma^{a,*}, Xiaohong Shu^{a,*}

^a College of Pharmacy, Dalian Medical University, Dalian 116044, PR China

^b School of Pharmaceutical Engineering, and Key Laboratory of Structure-Based Drug Design & Discovery (Ministry of Education), Shenyang Pharmaceutical University, Shenyang 110016, PR China

^c Department of Hematology, The First Affiliated Hospital of Dalian Medical University, Dalian 116011, PR China

^d Dalian Buyun Biotechnology Co., Ltd. 116085, PR China

ARTICLE INFO

Keywords:

B-cell lymphoma
JAK3 inhibitor
Thieno[3,2-*d*]pyrimidines

ABSTRACT

JAK3 is predominantly expressed in hematopoietic cells and has been a promising therapeutic target for the treatment of B-cell lymphoma. In this study, a new class of thieno[3,2-*d*]pyrimidines harboring acrylamide pharmacophore were synthesized as potent covalent JAK3 inhibitors ($IC_{50} < 10$ nM). Among them, **9a** and **9g** displayed the strongest inhibitory potency against JAK3 kinase activity, with IC_{50} values of 1.9 nM and 1.8 nM, respectively. Furthermore, compared with the reference agents, Spetrutinib and Ibrutinib, **9a** not only demonstrated enhanced antiproliferative activity against B lymphoma cells, but also showed very weak proliferative inhibition against normal peripheral blood mononuclear cells (PBMCs) at a concentration of 20 μ M. Analysis of the mechanism revealed that **9a** could induce the obvious apoptosis in B lymphoma cells and prevent JAK3-STAT3 cascade as well as BTK pathway. Taken together, **9a** may be served as a potential new JAK3 inhibitor for the treatment of B-cell lymphoma.

1. Introduction

Janus Kinase (JAK) is a family of non-receptor tyrosine kinases that transduce signal from transmembrane receptors to the nucleus and further modulate the transcription of target genes [1–3]. In mammalian, JAK family has four members: JAK1, JAK2, JAK3 and Tyk2 [4]. Unlike other JAKs that are ubiquitously expressed and associated with diverse cytokine receptors, JAK3 is predominantly expressed in hematopoietic cells and is induced by cytokine receptors that contain a common γ chain, such as receptors for interleukin2 (IL2), IL4, IL7, and IL21 [5,6]. After phosphorylation by a JAK, STAT forms hetero- or homo-dimers and is translocated to the cell nucleus, where it induces the transcription of target genes [7,8]. The JAK-STAT signaling pathway conveys the extracellular signals from various peptides, including many cytokines and chemokines as well as growth factors and hormones, directly to the nucleus to induce a variety of cellular responses, which is of fundamental importance in innate immunity, inflammation, and hematopoiesis, and dysregulation is frequently observed in immune disease and cancer. JAK3 also has been shown to play

an essential role in T lymphocyte development, proliferation and differentiation and its deficiency causes impaired T lymphocyte immunity, leading to severe combined immunodeficiency [9].

Various JAK inhibitors have been evaluated in clinical trials, including Tofacitinib (**1**) [10], Ruxolitinib (**2**) [11], Pacritinib (**3**) [12], CYT-387 (**4**) [13], AZD1480 (**5**) [14] and others [15] (Fig. 1). Recent studies have shown that the expression of JAK3 pathway genes are upregulated in different diagnostic classes of B-lineage lymphoid malignancies and are associated with the overexpression of genes for JAK3-activating cytokines [16,17]. It is different from the other JAKs, a unique cysteine residue (Cys909) locates in the gatekeeper-plus-7 (GK + 7) position of JAK3, which makes it possible to develop covalent binding inhibitors [18]. **6** [19], **7** [20] and **8** [21] have been reported as selective covalent JAK3 inhibitors. These findings have collectively identified JAK3 as an attractive molecular target for disrupting the constitutively active anti-apoptotic STAT3 and STAT5 signaling pathways in lymphoma cells.

In our continuous effort to discover potent EGFR^{T790M} and BTK inhibitors, we have identified several classes of pyrimidine derivatives

* Corresponding authors.

E-mail addresses: xiaodong.ma@139.com (X.D. Ma), xiaohong_shu@dlmedu.edu.cn (X.H. Shu).

¹ These authors contributed equally to this work.

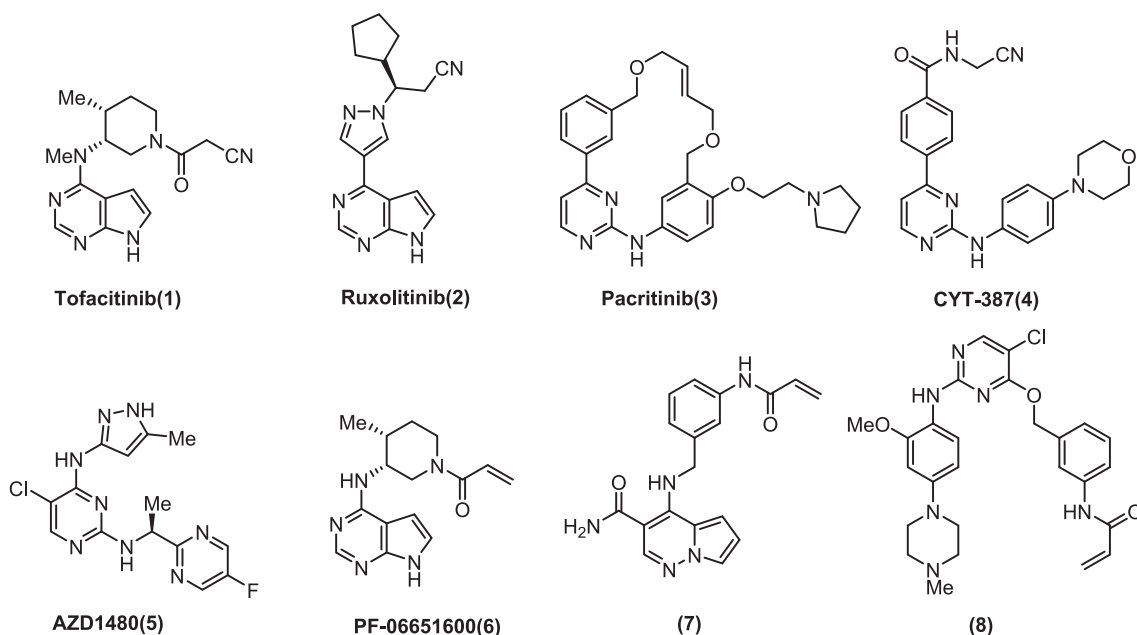


Fig. 1. The structures of potent JAK inhibitors.

as potential anticancer agents in our previous work [22–26]. Notably, the residue is Cys909 in human JAK3, and it is structurally similar to cysteine residues in EGFR (Cys797) and BTK (Cys481) that have been successfully targeted by covalent kinase inhibitors which are now approved drugs. Considering the structural similarity of the catalytic regions of these kinases, skillful structural transformation for the EGFR or BTK inhibitors may be a good protocol to discover new JAK3 inhibitors. The docking suggested that introduction of thiazole ring could come into closer contact with the gatekeeper Met902 in JAK3 to give enhanced interaction. We surmised that was a critical point for the exploration of selective JAK3 inhibitors. To investigate more effective JAK3 inhibitors, in this work, BTK inhibitor Spebrutinib as the lead, a family of thieno[3,2-*d*]pyrimidines harboring acrylamide pharmacophore was synthesized and systematical structural modification was carried out here (see Fig. 2). In addition, biological activity against JAK3 and B lymphoma cells *in vitro* were also investigated in detail in this study.

2. Results and discussion

2.1. Chemistry

The synthetic routes of the title compounds **9a–k** were depicted in Schemes 1–3. The commercially available starting material 3-amino-phenol (**10**) was reacted with acryloyl chloride to produce **11** which in the next step substituted the C-4 chloride atom in 2,4-dichlorothiopheno [3,2-*d*]pyrimidine to give the key intermediate **12**. Additionally, **13** was reacted with 1-bromo-3-chloropropane to synthesize **14**. Intermediate **14** was reacted with morpholine and then reduced by Fe-NH₄Cl reagent to get aniline **16**. The nucleophilic substitution reaction of the chlorine atom in **12** with **16** was occurred under the action of trifluoroacetic acid (TFA) to obtain the desired **9a** and **9b**. For the synthesis of **9c–i**, a condensation reaction was performed in the first step using the EDCI and HOBt; then, the desired **9c–i** was conveniently prepared *via* reduction and nucleophilic substitution reaction. The preparation of **9j–k** using the method below: 4-

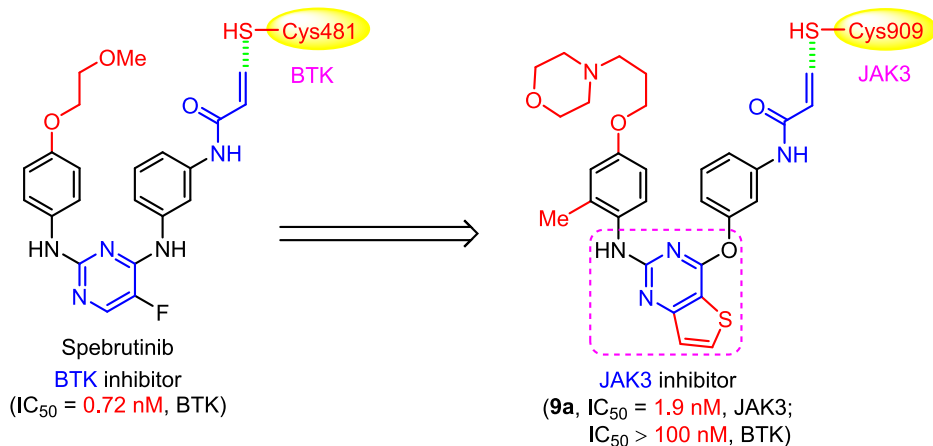
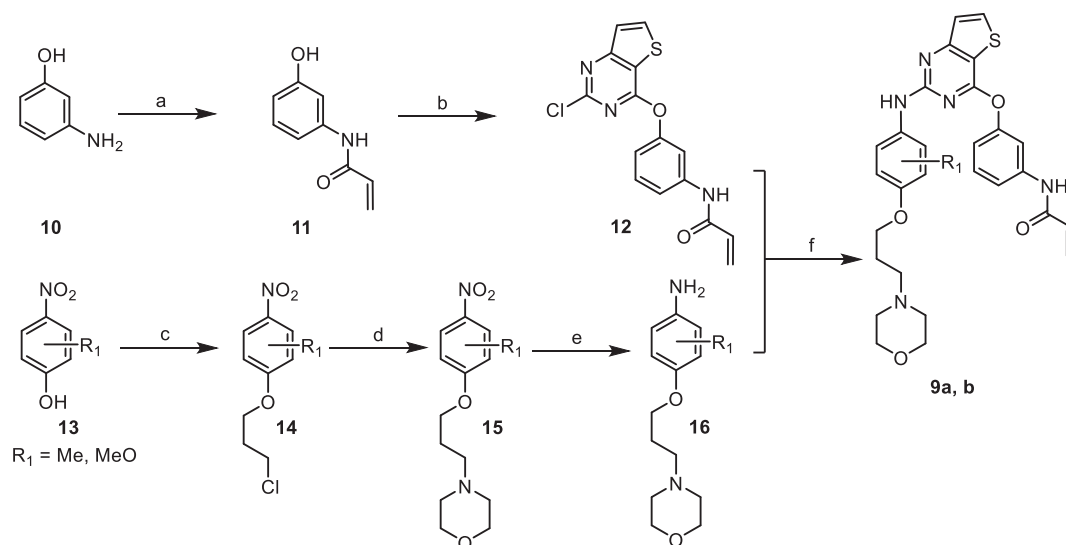


Fig. 2. Discovery strategy of the title molecules as JAK3 inhibitors.



Scheme 1. The synthetic route of 9a, b.

nitroaniline was reacted with bromoacetyl bromide to prepare the bromo-substituted **21**; then, through a nucleophilic substitution reaction with morpholine and a reduction reaction using Fe-NH₄Cl reagents, the aniline **23** was synthesized; additionally, in the presence of TFA, **23** was conveniently converted to the title molecules **9j–k** by reacting with **12**.

Reagents and conditions: (a) Acryloylchloride, NaHCO₃, CH₃CN, 0 °C, 0.5 h, 95%; (b) 2,4-dichlorothiopheno [3,2-*d*]pyrimidine, K₂CO₃, KI, DMF, 81%; (c) 1-bromo-3-chloropropane, K₂CO₃, CH₃CN, reflux, 12 h, 77–82%; (d) Morpholine, K₂CO₃, KI, DMF, 100 °C, 5 h, 72–85%; (e) Fe-NH₄Cl, MeOH-H₂O, 2 h, 70 °C, 66–70%; (f) Trifluoroacetic acid, 2-BuOH, 100 °C, 12 h, 9.3–21%.

Reagents and conditions: (a) Morpholine, EDCI, HOBT, rt, 12 h, 47–71%; (b) Fe-NH₄Cl, MeOH-H₂O, 2 h, 70 °C, 71–83%; (c) Trifluoroacetic acid, 2-BuOH, 100 °C, 12 h, 9–34%.

Reagents and conditions: (a) Bromoacetyl bromide, NaHCO₃, CH₃CN, rt, 5 h, 93–95%; (b) Morpholine, K₂CO₃, CH₃CN, reflux, 5 h, 85–90%; (c) Fe-NH₄Cl, MeOH-H₂O, 2 h, 70 °C, 73–81%; (d) Trifluoroacetic acid, 2-BuOH, 100 °C, 12 h, 12.6–21%.

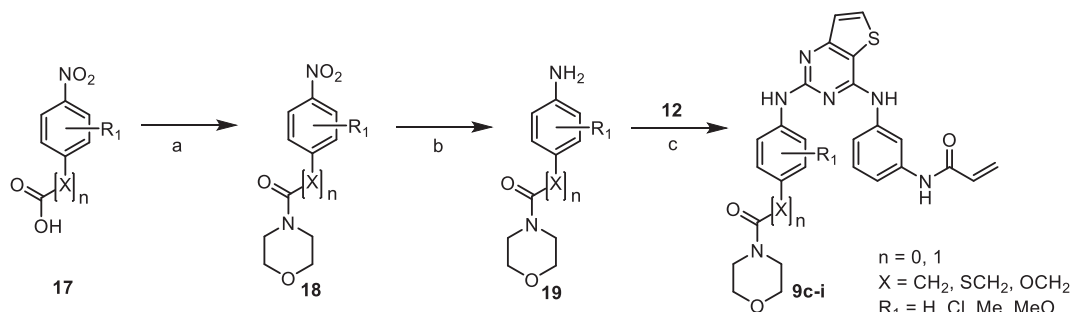
2.2. Biological activity

2.2.1. The inhibitory evaluation of kinase and cells proliferation

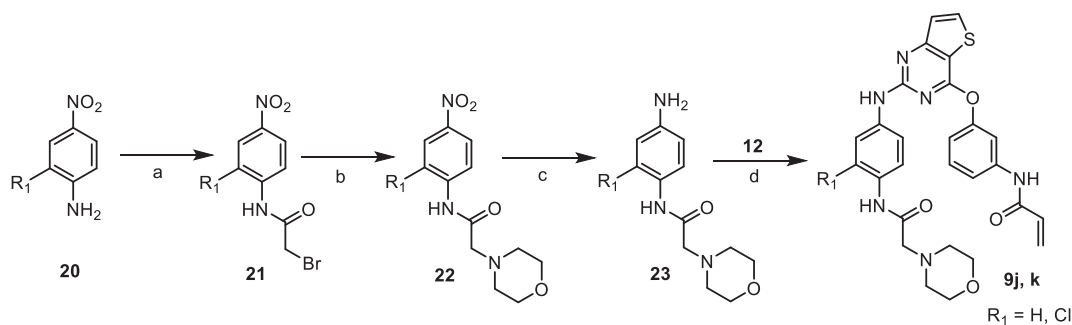
All these title molecules were evaluated for their inhibitory effects on JAK3. As shown in Table 1, most of the target compounds significantly inhibited the enzymatic activity with an IC₅₀ ranging from 1.8 to 568.9 nM among which **9a** (IC₅₀, 1.9 nM) and **9g** (IC₅₀, 1.8 nM) showed the strongest activity against JAK3. Regarding the structure and activity relationships, most of the introduced groups were favorable for the inhibition of JAK3. However, when a chlorine atom was introduced

into the C-3 aniline, the produced **9f** and **9k** showed about 38 and 250 times lower activity than that of **9d** and **9j**, respectively. On the other hand, the deletion of a methylene group in the aniline side chain of **9i** was beneficial to the inhibitory activity against JAK3. Overall, these work led to the successful identification of several thieno[3,2-*d*]pyrimidines with improved anti-JAK3 activity compared with reference agents.

These newly obtained thieno[3,2-*d*]pyrimidines were also evaluated for their capability to inhibit the proliferation of B lymphoma cell lines (Ramos, Raji and Namalwa). The results shown in Table 1 indicated that most of these compounds interfered with the proliferation of B lymphoma cells with IC₅₀ values lower than 20 μM. The representative **9b** displayed the strongest activity against both Ramos (IC₅₀, 9.7 μM) and Raji cells (IC₅₀, 5.3 μM), despite its moderate activity against JAK3 (IC₅₀, 95.2 nM). **9k** was the most potent inhibitor against Namalwa cells (IC₅₀, 6.2 μM), but only exhibited very weak activity against JAK3 (IC₅₀, 568.9 nM), suggesting that it may block the cell proliferation through a signaling pathway independent of JAK3. **9d** not only displayed strong activity against JAK3 (IC₅₀, 2.3 nM), but also effectively interfered with the proliferation of B lymphoma cells with IC₅₀ values lower than 15.1 μM. The cell-based test results showed that the short linker between the morpholine and phenyl was unfavorable for the inhibition of B lymphoma cells. The prototypical **9h** and **9i** showed reduced anti-proliferative activity against B lymphoma cells in this family of inhibitors. The results presented in Fig. 3 clearly indicated that **9a** exhibited a dose- and time-dependent inhibition of Ramos and Raji cells with concentrations ranging from 2.5 to 20 μM. In addition, the anti-proliferative activity of **9a** against B lymphoma cells (Ramos cells and Raji cells) was also evaluated by the acridine orange/ethidium bromide (AO/EB) staining assay (Fig. 4). After treatment with **9a** for



Scheme 2. The synthetic route of 9c-i.



Scheme 3. The synthetic route of 9j, k.

Table 1

Inhibitory activity against BTK, JAK3 and B lymphoma cells of 9a-k.^a

Compounds	R ₁	R ₂	Enzymatic activity (IC ₅₀ , nM) ^b		Antiproliferative activity (IC ₅₀ , μM) ^c			
			BTK	JAK3	Ramos	Raji	Namalwa	L-02
9a	2'-CH ₃		> 100.00	1.89 ± 0.04	10.44 ± 0.14	9.43 ± 0.14	9.92 ± 0.30	23.44 ± 0.08
9b	3'-OCH ₃		90.14 ± 0.04	95.21 ± 0.13	9.61 ± 0.44	5.32 ± 0.13	14.17 ± 0.37	10.27 ± 0.09
9c	H		80.32 ± 0.02	7.31 ± 0.08	13.51 ± 0.40	18.57 ± 0.27	14.39 ± 0.53	10.98 ± 0.11
9d	H		> 100.00	2.27 ± 0.04	15.11 ± 0.26	7.54 ± 0.22	9.73 ± 0.43	18.26 ± 0.30
9e	2'-CH ₃		33.60 ± 0.04	20.61 ± 0.05	19.00 ± 0.29	9.72 ± 0.24	19.53 ± 0.16	19.56 ± 0.25
9f	3'-Cl		25.28 ± 0.09	87.02 ± 0.16	18.57 ± 0.24	12.13 ± 0.31	14.63 ± 0.56	11.93 ± 0.13
9g	3'-OCH ₃		19.96 ± 0.28	1.78 ± 0.06	19.66 ± 0.11	9.90 ± 0.11	18.91 ± 0.13	18.28 ± 0.19
9h	H		> 100.00	2.13 ± 0.13	29.08 ± 0.31	> 40.00	22.63 ± 0.45	16.51 ± 0.38
9i	H		> 100.00	460.20 ± 0.09	28.22 ± 0.41	28.92 ± 0.46	12.37 ± 0.22	14.88 ± 0.07
9j	H		24.05 ± 0.47	8.77 ± 0.07	20.36 ± 0.67	19.76 ± 0.11	14.51 ± 0.42	3.10 ± 0.06
9k	3'-Cl		> 100.00	568.90 ± 0.03	18.14 ± 0.30	18.66 ± 0.20	6.23 ± 0.53	6.46 ± 0.12
Spebrutinib			0.72 ± 0.04	66.54 ± 0.04	14.62 ± 0.40	19.14 ± 0.09	18.72 ± 0.41	< 2.50
Ibrutinib			0.34 ± 0.03	16.11 ± 0.07	5.01 ± 0.11	10.42 ± 0.14	9.63 ± 0.38	10.87 ± 0.15

^a Data represent the mean of at least three separate experiments, the exact concentrations for cytotoxic studies were 1.25 μM, 5 μM, 10 μM, 20 μM and 40 μM.

^b Dose-response curves were determined at five concentrations. The IC₅₀ values are the concentrations in nanomolar needed to inhibit cell growth by 50% as determined from these curves.

^c Dose-response curves were determined at five concentrations. The IC₅₀ values are the concentrations in micromolar needed to inhibit cell growth by 50% as determined from these curves.

48 h, the proliferation of B lymphoma cells was markedly blocked at concentration below 20 μM, which was not the case with Spebrutinib.

2.2.2. Cell cytotoxicity evaluation

The effects of 9a on the viability of Ramos, Raji, Namalwa cells and L-02 cells were evaluated by cck-8 method (Fig. 5). With the increasing of the concentrations of 9a, the viability of Ramos, Raji, Namalwa cells decreased suddenly. When 9a inhibited B lymphoma cells by a half, L-02 still remained high viability. Meanwhile, the cell cytotoxicity of 9a against normal peripheral blood mononuclear cells (PBMCs) was also evaluated by the AO/EB staining assay (Fig. 6). Clearly, 9a did not significantly inhibit the proliferation of PBMCs at a concentration of 20 μM as well as the approved kinase inhibitor Spebrutinib. The results of cytotoxic evaluation showed that 9a possessed less effect on cells line

than that of Spebrutinib. Taken together, these findings indicated that 9a could serve as a promising JAK inhibitor for the treatment of B-cell lymphoma after further biological evaluations.

2.2.3. Flow cytometry analysis

In addition, to further investigate the antiproliferative mechanism of these inhibitors against B lymphoma cells, the effects of the most active inhibitor 9a on apoptosis and on the cell cycle in Ramos cell line were also examined using flow cytometry analysis. For comparison, Spebrutinib was also evaluated as the reference compound. The results presented in Fig. 7 revealed that 9a induced apoptosis in Ramos cells in a dose- and time-dependent manner. Additionally, the apoptosis rate increased from 19.1 to 49.2% after 48 h with increasing concentration from 5 to 10 μM. Treatment with identical concentration (20 μM) of

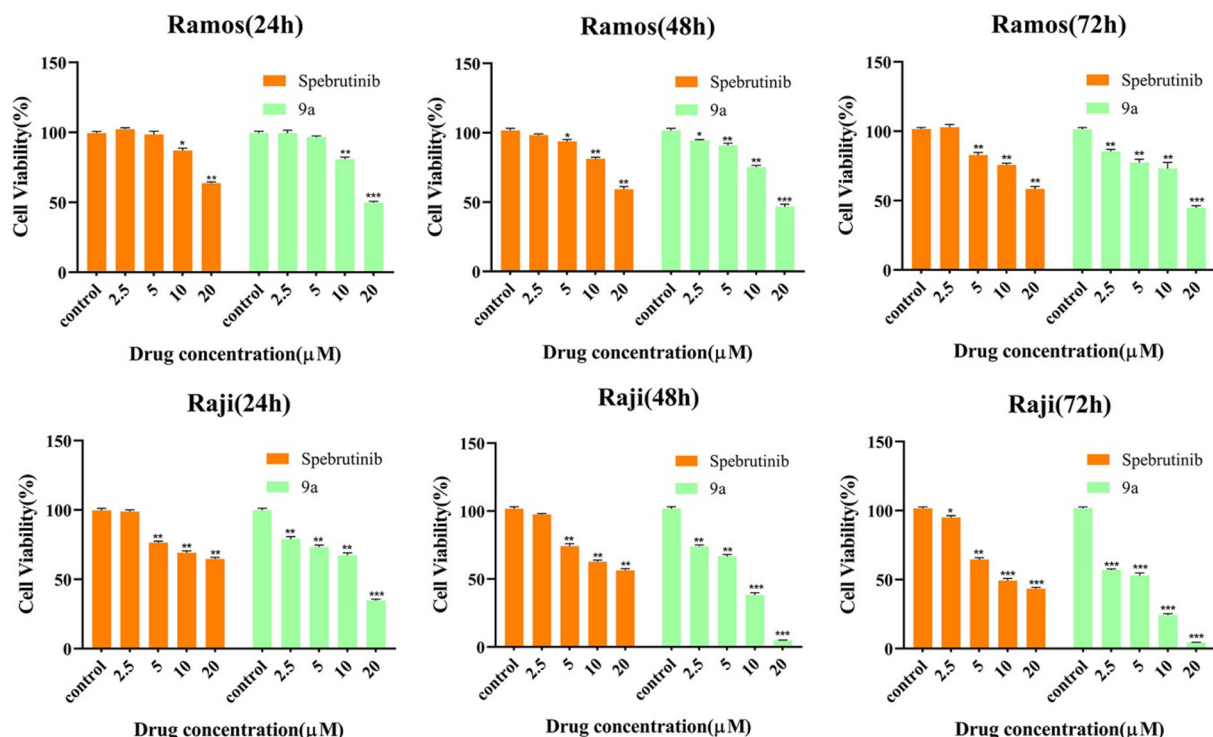


Fig. 3. The effects of treating time and concentration of **9a** against B lymphoma cells (Ramos cells and Raji cells). * $p < 0.05$, ** $p < 0.01$, *** $p < 0.001$ compared with control group.

Spebrutinib and **9a** for 48 h, Ramos cells obtained 44.1 and 78.2% loss of cell viability, respectively. The effects of **9a** on the cell-cycle progression of Ramos cells were shown in Fig. 8. Incubation with **9a** at concentrations from 5 to 20 μM for 48 h, compared with the control group, the percentage of Ramos cells in the G2/M phase increased from 20.4 to 38.9%, and those in the G0/G1 decreased from 51.9 to 35.5%. Apparently, the newly synthesized **9a** blocked the cell cycle in Ramos cells at the G2/M phase.

2.2.4. Effects of the inhibitors on BTK and JAK3 activation and downstream signaling

To gain a better insight into the underlying mechanism of JAK3 inhibitors, the inhibitory effects of **9a** on the JAK-STAT3 activation and downstream signaling were examined in Namalwa cells using Spebrutinib as a comparison control. In addition, considering that BTK protein was also highly expressed in Namalwa cells, the effects of **9a** on BTK activation were also evaluated. The cells were treated with different concentrations (5, 10, 20 μM) of inhibitors for 24 h, and the levels of STAT3, p-STAT3, BTK and p-BTK was determined by immune blotting analysis. The results summarized in Fig. 9 revealed that the phosphorylation of STAT3 which located downstream of the signaling pathway was inhibited by **9a** in Namalwa cells in a dose-dependent manner. **9a** was also found to clearly downregulated the expression of p-BTK. These results indicated that **9a** could block the phosphorylation of STAT3 and then restrain the activation of the signaling pathway.

2.2.5. Molecular modeling analysis

To determine the relationship between the inhibitory effect of the title molecules against JAK3 and their binding models with JAK3, four representative compounds, namely **9a**, **9g**, **9k** and **9i**, were individually docked into the binding pocket of the JAK3 protein. Similarly, Spebrutinib was also docked into the binding pocket. The crystal structure of the prototypical molecule **8** with JAK3 protein was used for comparison. The AutoDock 4.2 software (The Scripps Research Institute, La Jolla, CA, USA) and its default parameters were used for

molecular docking performance. As depicted in Fig. 10 A-D, all the four potent JAK3 inhibitors could form a potential covalent bond between the acrylamide and Cys909 in the JAK3 protein. However, for the weaker inhibitors **9k** (Fig. 10 E) and **9i** (Fig. 10 F), this important bond disappeared due to the long distance ($> 10.10 \text{ \AA}$) between the acrylamide group and the Cys909 residue. Clearly, the acrylamide group and morpholine substrate in both **9k** and **9i** were in the opposite position in the JAK3 binding pocket, thus resulting in a long distance. Notably, for **9a** (Fig. 10 D) and **9g** (Fig. 10 C), the newly introduced thiazole ring could come into closer contact with Met902 than that in Spebrutinib, which possibly led to the higher anti-JAK3 activity. In short, these binding models reasonably explained their activity against JAK3.

3. Conclusion

JAK3 is an important therapeutic target for the treatment of B-cell lymphoma. Targeting JAK3 may result in several outstanding advantages in the treatment of malignant tumors, including improved therapeutic efficacy, safety and resistance profiles by collective regulations of a primary therapeutic target together with compensatory elements and resistance activities. In this study, several potent JAK3 inhibitors were identified and evaluated for the treatment of B-cell lymphoma. Most of these compounds displayed strong inhibitory effects against JAK3 at concentrations below 10 nM. In particular, **9a** and **9g** were the strongest JAK3 inhibitors in this class of kinase inhibitors, with IC_{50} values less than 2 nM. In addition, the cell-based assay results revealed that **9a** exhibited enhanced anticancer activity compared with the reference agents. Additionally, the normal PBMCs were found to be not sensitive to **9a**, indicating its low cell cytotoxicity. Furthermore, analysis of the mechanism of these compounds revealed that **9a** induced significant apoptosis in Ramos cells by arresting the cell cycle at G2/M stage and blocked JAK3-STAT3 cascade. Overall, these newly discovered JAK3 inhibitors are of great therapeutic value and warrant further study as potential agents for the treatment of B-cell lymphoma.

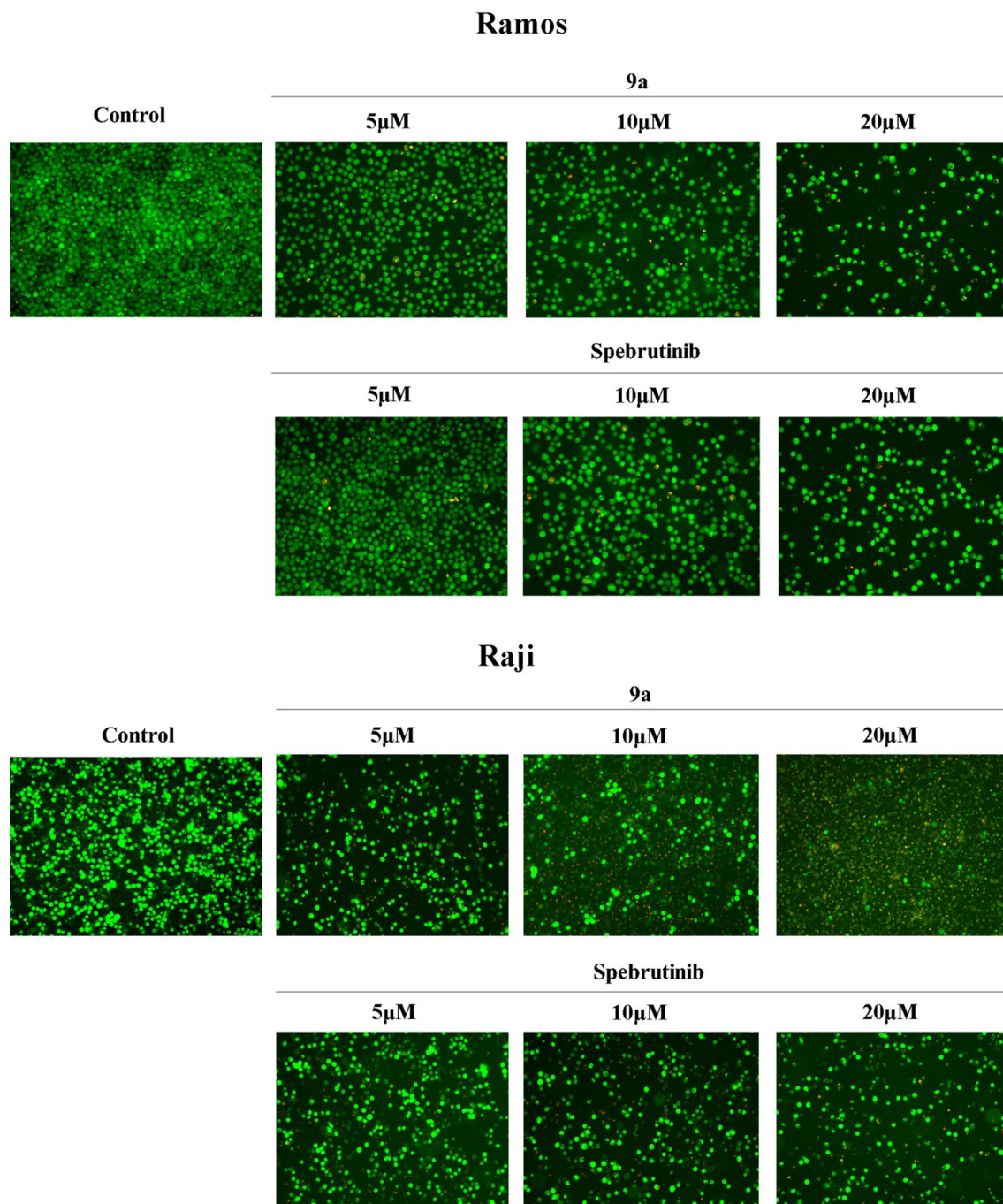


Fig. 4. Morphological changes of the Ramos, Raji cells treated by **9a** (200 \times , final magnification) at concentrations of 5, 10, 20 μ M for 48 h.

4. Experimental section

4.1. General methods for chemistry

Unless otherwise indicated, all reagents and solvents were obtained from commercial sources and used as received. ^1H and ^{13}C NMR data were obtained on a Bruker Avance at 400 and 100 MHz, respectively. Coupling constants (J) are expressed in hertz (Hz). Chemical shifts (δ) of NMR are reported in parts per million (ppm) units relative to internal control (TMS). High resolution ESI-MS was performed on an AB Sciex Triple TOF[®] 4600 LC/MS/MS system. All reactions were monitored by TLC, using silica gel plates with fluorescence F254 and UV light visualization. Flash chromatography separations were obtained on Silica Gel (300–400 mesh) using dichloromethane/methanol as eluents.

4.2. General procedure for the synthesis of **9a–k**

4-Morpholine-substituted aniline intermediates **12**, **16**, **19**, **23** were generally prepared referencing the procedures showed in literatures [22–26]. All these intermediates were directly used without any purification and structural characterization. With these intermediates in hand, the desired compounds were synthesized as described below. A flask was charged with **12** (0.70 mmol), anilines **16**, **19**, **23** (0.70 mmol), TFA (1.05 mmol), and 2-BuOH (10 mL). The slurry was heated to 100 $^\circ\text{C}$ for 5 h. The reaction mixture was allowed to cool to room temperature and was neutralized with a saturated aqueous sodium bicarbonate solution. The aqueous mixture was then extracted with CH_2Cl_2 (20 mL) three times. The crude product was purified using flash chromatography with dichloromethane/methanol (v/v, 30:1) as eluents.

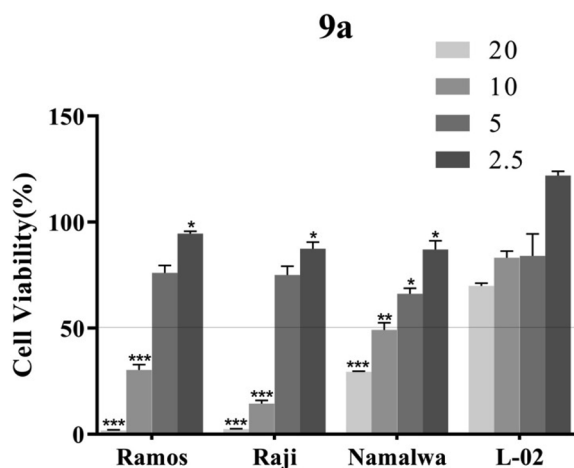


Fig. 5. The effects of treating for 72 h by **9a** on B lymphoma cells (Ramos, Raji and Namalwa cells) and human normal liver cells (L-02 cells). * $p < 0.05$, ** $p < 0.01$, *** $p < 0.001$ compared with L-02 group.

4.2.1. *N*-(3-(2-(4-(3-morpholinopropoxy)-2-methylphenylamino)thieno[3,2-*d*]pyrimidin-4-yloxy) phenyl)acrylamide (**9a**)

Yield 9.3%; off-white solid. $^1\text{H NMR}$ (DMSO- d_6): δ 10.33 (s, 1H), 8.50 (s, 1H), 8.20 (d, $J = 5.4$ Hz, 1H), 7.71 (t, $J = 2.0$ Hz, 1H), 7.54 (d, $J = 8.2$ Hz, 1H), 7.41 (t, $J = 8.2$ Hz, 1H), 7.22 (d, $J = 5.4$ Hz, 1H), 7.19 (d, $J = 8.7$ Hz, 1H), 7.05 (dd, $J = 8.2, 2.0$ Hz, 1H), 6.73 (d, $J = 2.6$ Hz, 1H), 6.60 (dd, $J = 8.7, 2.6$ Hz, 1H), 6.46 (dd, $J = 17.0, 10.1$ Hz, 1H), 6.28 (dd, $J = 17.0, 1.9$ Hz, 1H), 5.79 (dd, $J = 10.1, 1.9$ Hz, 1H), 3.95 (t, $J = 6.8$ Hz, 2H), 2.58 (t, $J = 4.6$ Hz, 4H), 2.42 (t, $J = 6.8$ Hz, 2H), 2.40–2.32 (m, 4H), 2.13 (s, 3H), 1.85 (qui, $J = 6.8$ Hz, 2H); $^{13}\text{C NMR}$ (DMSO- d_6): δ 165.6, 164.0, 163.8, 160.1, 156.0, 152.6, 140.7, 136.9, 134.8, 132.1, 131.3, 130.3, 127.8, 127.4, 123.6, 117.4, 116.9, 116.3, 113.2, 112.0, 107.3, 66.7 (2C), 66.2, 55.3, 53.8 (2C), 26.4, 18.8; HRMS (ESI) for $\text{C}_{29}\text{H}_{31}\text{N}_5\text{O}_4\text{S}$, $[\text{M}+\text{H}]^+$ calcd: 546.2170, found: 546.2155.

4.2.2. *N*-(3-(2-(4-(3-morpholinopropoxy)-3-methoxyphenylamino)thieno[3,2-*d*]pyrimidin-4-yloxy) phenyl)acrylamide (**9b**)

Yield 23.3%; Pale-yellow solid. $^1\text{H NMR}$ (DMSO- d_6): δ 10.46 (s, 1H), 9.29 (s, 1H), 8.28 (d, $J = 5.3$ Hz, 1H), 7.73 (s, 1H), 7.60 (d, $J = 8.1$ Hz, 1H), 7.44 (t, $J = 8.1$ Hz, 1H), 7.38 (s, 1H), 7.35 (d, $J = 5.3$ Hz, 1H), 7.19 (d, $J = 8.6$ Hz, 1H), 7.07 (d, $J = 8.1$ Hz, 1H), 6.76 (d, $J = 8.6$ Hz, 1H), 6.47 (dd, $J = 16.8, 10.1$ Hz, 1H), 6.24 (dd, $J = 16.8, 2.0$ Hz, 1H), 5.77 (dd, $J = 10.1, 2.0$ Hz, 1H), 3.94 (t, $J = 5.72$ Hz, 2H), 3.84–3.73 (m, 4H), 3.61 (s, 3H), 3.42–3.36 (m, 2H), 3.16–3.05 (m, 4H), 2.10–1.98

(m, 2H); $^{13}\text{C NMR}$ (DMSO- d_6): δ 165.1, 164.0, 163.9, 158.3, 152.7, 149.5, 142.7, 140.9, 137.3, 135.5, 132.1, 130.4, 127.8, 123.7, 117.3, 117.1, 115.0, 113.2, 111.2, 108.1, 105.0, 67.3, 64.4 (2C), 55.8, 54.6, 52.1 (2C), 24.4; HRMS (ESI) for $\text{C}_{28}\text{H}_{27}\text{N}_5\text{O}_6\text{S}$, $[\text{M}+\text{H}]^+$ calcd: 562.2119, found: 562.2127.

4.2.3. *N*-(3-(2-(4-((1-morpholino)acetylthio)phenylamino)thieno[3,2-*d*]pyrimidin-4-yloxy)phenyl) acrylamide (**9c**)

Yield 15.6%; off-white solid. $^1\text{H NMR}$ (DMSO- d_6): δ 10.38 (s, 1H), 9.61 (s, 1H), 8.33 (d, $J = 5.4$ Hz, 1H), 7.75 (t, $J = 2.3$ Hz, 1H), 7.62 (d, $J = 8.1$ Hz, 1H), 7.59 (d, $J = 8.8$ Hz, 2H), 7.49 (t, $J = 8.1$ Hz, 1H), 7.39 (d, $J = 5.4$ Hz, 1H), 7.21 (d, $J = 8.8$ Hz, 2H), 7.10 (dd, $J = 8.1, 2.3$ Hz, 1H), 6.45 (dd, $J = 17.0, 10.1$ Hz, 1H), 6.27 (dd, $J = 17.0, 2.0$ Hz, 1H), 5.79 (dd, $J = 10.1, 2.0$ Hz, 1H), 3.80 (s, 2H), 3.55–3.50 (m, 4H), 3.45–3.39 (m, 4H); $^{13}\text{C NMR}$ (DMSO- d_6): δ 167.1, 165.1, 164.2, 163.8, 157.9, 152.7, 140.8, 140.3, 137.6, 132.1, 131.8 (2C), 130.5, 127.8, 125.9, 123.7, 119.5 (2C), 117.6, 117.2, 113.4, 108.4, 66.5 (2C), 46.6, 42.2, 37.2; HRMS (ESI) for $\text{C}_{27}\text{H}_{25}\text{N}_5\text{O}_4\text{S}_2$, $[\text{M}+\text{H}]^+$ calcd: 548.1421, found: 548.1411.

4.2.4. *N*-(3-(2-(4-((1-morpholino)acetoxyl)phenylamino)thieno[3,2-*d*]pyrimidin-4-yloxy)phenyl)acrylamide (**9d**)

Yield 23.1%; Pale-yellow solid. $^1\text{H NMR}$ (DMSO- d_6): δ 10.36 (s, 1H), 9.31 (s, 1H), 8.28 (d, $J = 5.4$ Hz, 1H), 7.73 (t, $J = 2.2$ Hz, 1H), 7.61 (d, $J = 8.1$ Hz, 1H), 7.50 (d, $J = 8.6$ Hz, 2H), 7.45 (t, $J = 8.1$ Hz, 1H), 7.34 (d, $J = 5.4$ Hz, 1H), 7.09 (dd, $J = 8.1, 2.2$ Hz, 1H), 6.73 (d, $J = 8.6$ Hz, 2H), 6.45 (dd, $J = 17.0, 10.1$ Hz, 1H), 6.28 (dd, $J = 17.0, 2.0$ Hz, 1H), 5.79 (dd, $J = 10.1, 2.0$ Hz, 1H), 4.72 (s, 2H), 3.63–3.54 (m, 4H), 3.49–3.44 (m, 4H); $^{13}\text{C NMR}$ (DMSO- d_6): δ 166.7, 165.3, 164.1, 163.8, 158.3, 153.1, 152.7, 140.8, 137.3, 134.6, 132.1, 130.4, 127.8, 123.7, 120.7 (2C), 117.6, 117.1, 114.8 (2C), 113.4, 107.7, 66.7, 66.5 (2C), 45.3, 42.1; HRMS (ESI) for $\text{C}_{27}\text{H}_{25}\text{N}_5\text{O}_5\text{S}$, $[\text{M}+\text{H}]^+$ calcd: 532.1649, found: 532.1635.

4.2.5. *N*-(3-(2-(4-((1-morpholino)acetoxyl)-2-methylphenylamino)thieno[3,2-*d*]pyrimidin-4-yloxy) phenyl)acrylamide (**9e**)

Yield 9.3%; off-yellow solid. $^1\text{H NMR}$ (DMSO- d_6): δ 10.33 (s, 1H), 8.52 (s, 1H), 8.20 (d, $J = 5.4$ Hz, 1H), 7.77 (t, $J = 2.3$ Hz, 1H), 7.54 (d, $J = 8.1$ Hz, 1H), 7.42 (t, $J = 8.1$ Hz, 1H), 7.24 (d, $J = 5.4$ Hz, 1H), 7.20 (d, $J = 8.7$ Hz, 1H), 7.07 (dd, $J = 8.1, 2.3$ Hz, 1H), 6.76 (d, $J = 3.0$ Hz, 1H), 6.63 (dd, $J = 8.7, 3.0$ Hz, 1H), 6.45 (dd, $J = 16.9, 10.1$ Hz, 1H), 6.28 (dd, $J = 16.9, 2.0$ Hz, 1H), 5.79 (dd, $J = 10.1, 2.0$ Hz, 1H), 3.66–3.56 (m, 4H), 3.50–3.44 (m, 4H), 2.13 (s, 3H); $^{13}\text{C NMR}$ (DMSO- d_6): δ 166.6, 165.6, 164.1, 163.8, 160.1, 155.4, 152.6, 140.7, 136.9, 134.8, 132.1, 131.8, 130.3, 127.8, 127.4, 123.6, 117.4, 116.9, 116.4, 113.2, 112.2, 107.4, 66.5 (2C), 66.5, 45.3, 42.1, 18.8;

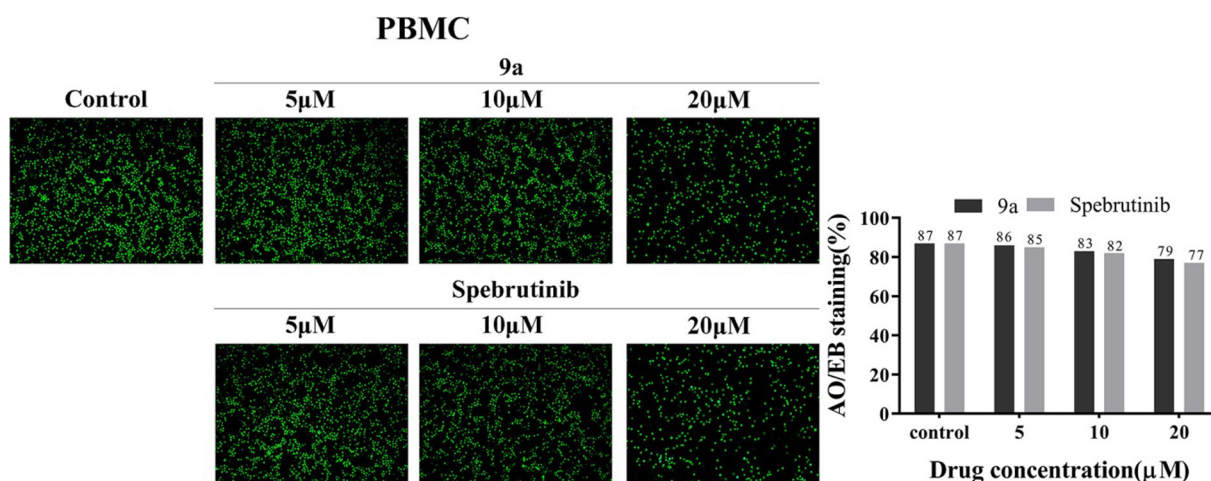


Fig. 6. Morphological changes of the PBMC cells treated by **9a** (200 \times , final magnification) at concentrations of 5, 10, 20 μM for 24 h.

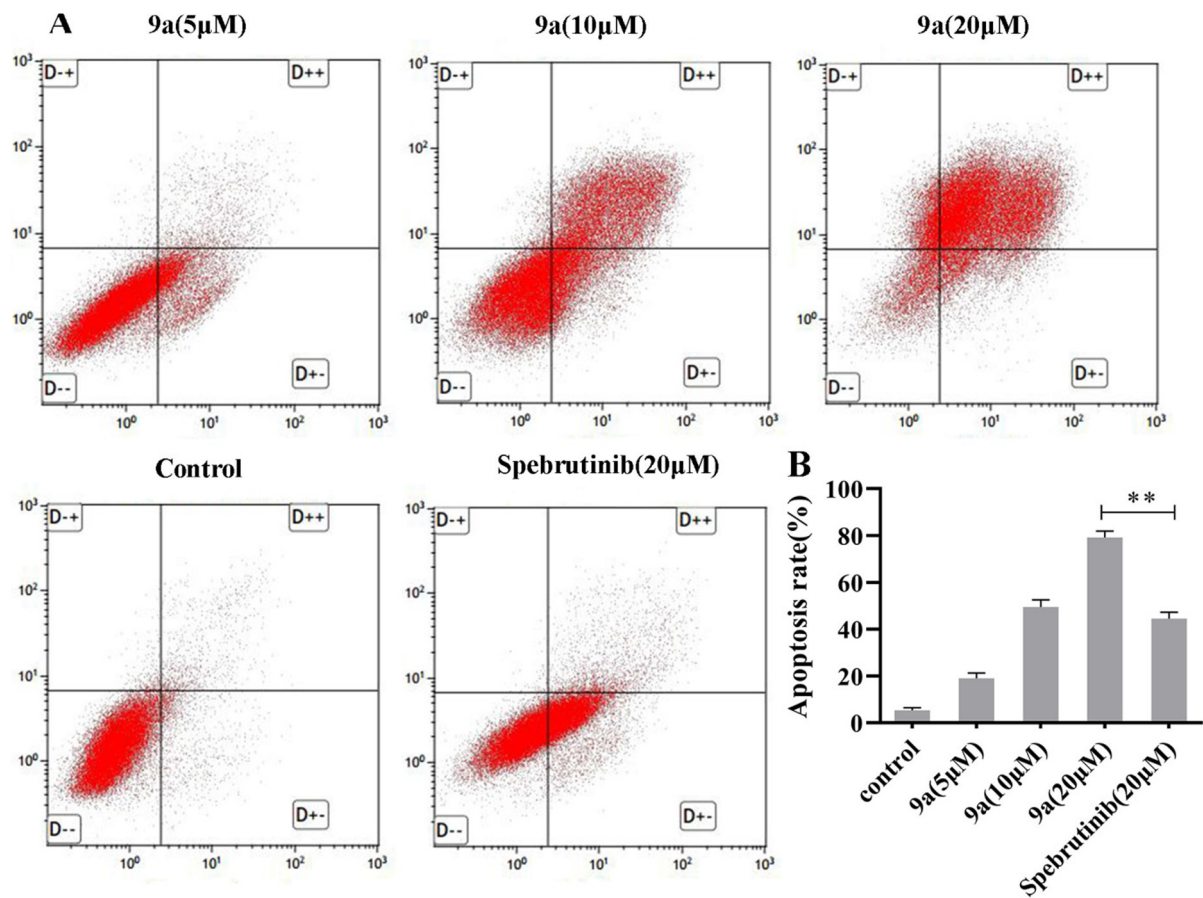


Fig. 7. **9a** induced Ramos cells apoptosis *in vitro*. The cells were incubated with the indicated concentrations of **9a** for 48 h, and the cells were stained with annexin V/FITC, followed by flow cytometry analysis. One representative experiment was shown. ** $p < 0.01$ compared with Spebrutinib group.

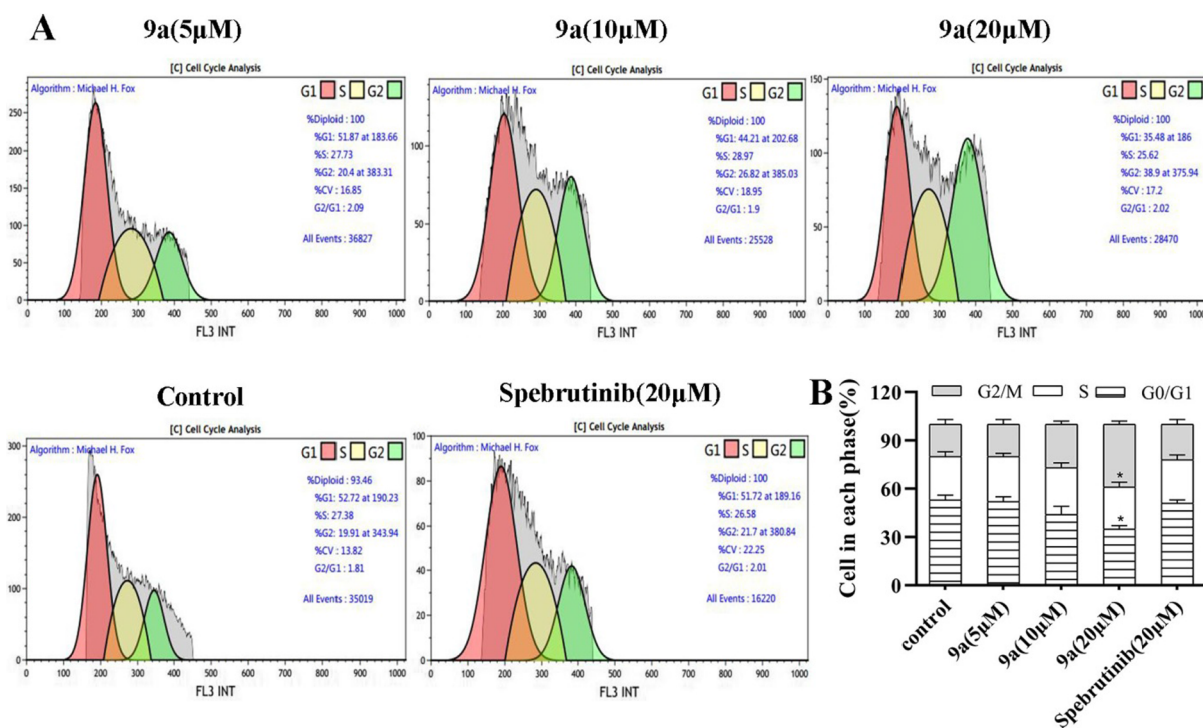


Fig. 8. Cell cycle arrest of the cells induced by **9a** was determined by flow cytometric analysis. One representative experiment is shown. * $p < 0.05$ compared with control group.

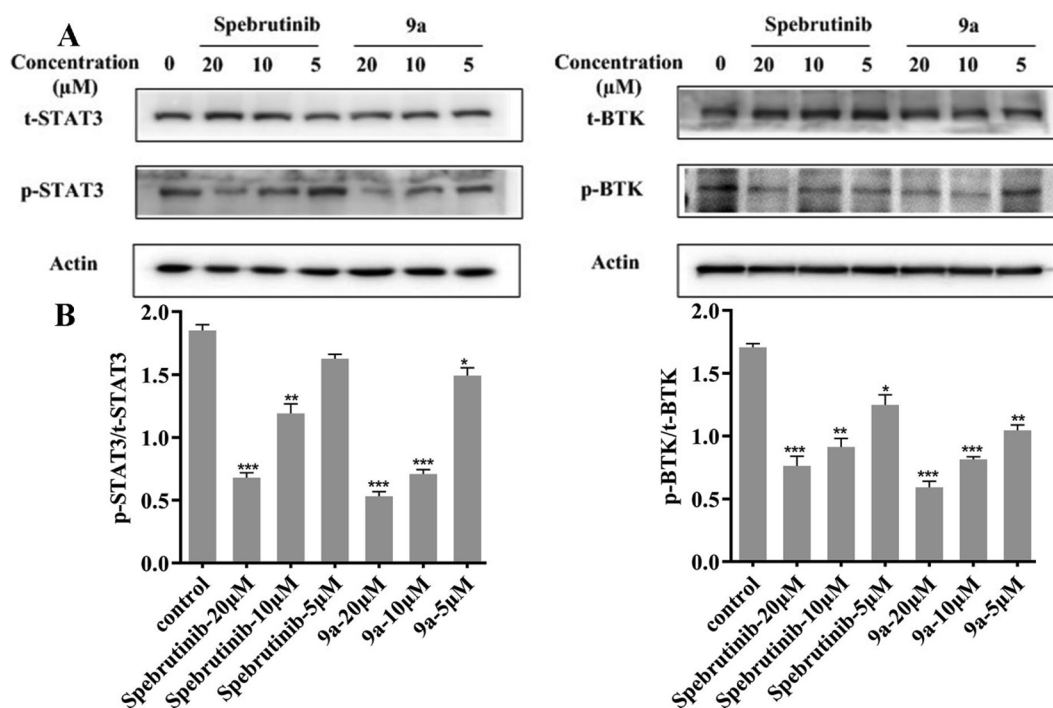


Fig. 9. (A) **9a** inhibited the activation of BTK and JAK-STAT3 signaling in Namalwa cells. (B) Gray intensity analysis of the Western blots, * $p < 0.05$, ** $p < 0.01$, *** $p < 0.001$ compared with control group.

HRMS (ESI) for $C_{28}H_{27}N_5O_5S$, $[M+H]^+$ calcd: 546.1806, found: 546.1790.

4.2.6. *N*-(3-(2-(4-((1-morpholino)acetoxyl)-3-chlorophenylamino)thieno[3,2-*d*]pyrimidin-4-yloxy)phenyl)acrylamide (**9f**)

Yield 15.1%; off-white solid. 1H NMR (DMSO- d_6): δ 10.35 (s, 1H), 9.48 (s, 1H), 8.31 (d, $J = 5.3$ Hz, 1H), 7.76 (s, 1H), 7.73 (t, $J = 2.2$ Hz, 1H), 7.60 (dd, $J = 8.1, 2.2$ Hz, 1H), 7.47 (t, $J = 8.1$ Hz, 1H), 7.45 (d, $J = 9.1$ Hz, 1H), 7.38 (d, $J = 5.3$ Hz, 1H), 7.09 (dd, $J = 8.1, 2.2$ Hz, 1H), 6.86 (d, $J = 9.1$ Hz, 1H), 6.44 (dd, $J = 17.0, 10.1$ Hz, 1H), 6.27 (dd, $J = 17.0, 2.0$ Hz, 1H), 5.78 (dd, $J = 10.1, 2.0$ Hz, 1H), 4.84 (s, 2H), 3.64–3.56 (m, 4H), 3.49–3.43 (m, 4H); ^{13}C NMR (DMSO- d_6): δ 166.2, 165.0, 164.1, 163.8, 158.0, 152.6, 148.3, 140.9, 137.5, 135.3, 132.1, 130.5, 127.8, 123.7, 121.2, 120.5, 118.7, 117.4, 117.3, 114.4, 113.1, 108.3, 67.3, 66.5 (2C), 45.3, 42.1; HRMS (ESI) for $C_{27}H_{24}ClN_5O_5S$, $[M+H]^+$ calcd: 566.1259, found: 566.1265.

4.2.7. *N*-(3-(2-(4-((1-morpholino)acetoxyl)-3-methoxyphenylamino)thieno[3,2-*d*]pyrimidin-4-yloxy)phenyl)acrylamide (**9g**)

Yield 33.3%; Pale-yellow solid. 1H NMR (DMSO- d_6): δ 10.35 (s, 1H), 9.29 (s, 1H), 8.29 (d, $J = 5.4$ Hz, 1H), 7.71 (t, $J = 2.2$ Hz, 1H), 7.59 (dd, $J = 8.1, 2.2$ Hz, 1H), 7.45 (t, $J = 8.1$ Hz, 1H), 7.38 (s, 1H), 7.37 (d, $J = 5.4$ Hz, 1H), 7.18 (d, $J = 8.8$ Hz, 1H), 7.09 (dd, $J = 8.1, 2.2$ Hz, 1H), 6.72 (d, $J = 8.8$ Hz, 1H), 6.44 (dd, $J = 16.8, 10.1$ Hz, 1H), 6.27 (dd, $J = 16.8, 2.0$ Hz, 1H), 5.79 (dd, $J = 10.1, 2.0$ Hz, 1H), 4.67 (s, 2H), 3.63 (s, 1H), 3.61–3.55 (m, 4H), 3.51–3.43 (m, 4H); ^{13}C NMR (DMSO- d_6): δ 166.7, 165.1, 164.0, 163.8, 158.3, 152.7, 149.4, 142.4, 140.8, 137.3, 135.6, 132.1, 130.4, 127.8, 123.8, 117.4, 117.1, 115.1, 113.1, 111.1, 108.1, 105.1, 68.2, 66.6 (2C), 55.9, 45.5, 42.1; HRMS (ESI) for $C_{28}H_{27}N_5O_6S$, $[M+H]^+$ calcd: 562.1755, found: 562.1755.

4.2.8. *N*-(3-(2-(4-(morpholinoformyl)phenylamino)thieno[3,2-*d*]pyrimidin-4-yloxy)phenyl)acrylamide (**9h**)

Yield 24.3%; White solid. 1H NMR (DMSO- d_6): δ 10.38 (s, 1H), 9.79 (s, 1H), 8.35 (d, $J = 5.4$ Hz, 1H), 7.78 (t, $J = 2.2$ Hz, 1H), 7.65 (d, $J = 8.6$ Hz, 2H), 7.61 (d, $J = 8.1$ Hz, 1H), 7.49 (t, $J = 8.1$ Hz, 1H), 7.41 (d, $J = 5.4$ Hz, 1H), 7.18 (d, $J = 8.6$ Hz, 2H), 7.11 (d, $J = 8.1$,

2.2 Hz, 1H), 6.44 (dd, $J = 16.8, 10.1$ Hz, 1H), 6.27 (dd, $J = 16.8, 2.0$ Hz, 1H), 5.79 (dd, $J = 10.1, 2.0$ Hz, 1H), 3.64–3.54 (m, 4H), 3.54–3.37 (m, 4H); HRMS (ESI) for $C_{26}H_{23}N_5O_4S$, $[M+H]^+$ calcd: 502.1544, found: 502.1533.

4.2.9. *N*-(3-(2-(4-(morpholinoacetyl)phenylamino)thieno[3,2-*d*]pyrimidin-4-yloxy)phenyl)acrylamide (**9i**)

Yield 29.8%; off-white solid. 1H NMR (DMSO- d_6): δ 10.37 (s, 1H), 9.49 (s, 1H), 8.31 (d, $J = 5.4$ Hz, 1H), 7.74 (t, $J = 2.2$ Hz, 1H), 7.61 (dd, $J = 8.1, 2.2$ Hz, 1H), 7.54 (d, $J = 8.1$ Hz, 2H), 7.47 (t, $J = 8.1$ Hz, 1H), 7.38 (d, $J = 5.4$ Hz, 1H), 7.10 (d, $J = 8.1, 2.2$ Hz, 1H), 6.97 (d, $J = 8.2$ Hz, 2H), 6.44 (dd, $J = 16.9, 10.1$ Hz, 1H), 6.27 (dd, $J = 16.9, 2.0$ Hz, 1H), 5.79 (dd, $J = 10.1, 2.0$ Hz, 1H), 3.59 (s, 2H), 3.54–3.49 (m, 4H), 3.47–3.42 (m, 4H); ^{13}C NMR (DMSO- d_6): δ 169.7, 165.2, 164.1, 163.8, 158.2, 152.7, 140.8, 139.3, 137.4, 132.1, 130.4, 129.1 (2C), 128.6, 127.8, 123.7, 119.1 (2C), 117.6, 117.1, 113.3, 108.0, 66.5 (2C), 46.4, 42.1, 39.2; HRMS (ESI) for $C_{27}H_{25}N_5O_4S$, $[M+H]^+$ calcd: 516.1700, found: 516.1692.

4.2.10. *N*-(3-(2-(4-((1-morpholino)acetyl)amino)-phenylamino)thieno[3,2-*d*]pyrimidin-4-yloxy)phenyl)acrylamide (**9j**)

Yield 20.1%; Pale-yellow solid. 1H NMR (DMSO- d_6): δ 10.34 (s, 1H), 9.52 (s, 1H), 9.41 (s, 1H), 8.29 (d, $J = 5.3$ Hz, 1H), 7.72 (s, 1H), 7.59 (d, $J = 8.2$ Hz, 1H), 7.53 (d, $J = 8.2$ Hz, 2H), 7.46 (t, $J = 8.2$ Hz, 1H), 7.37–7.36 (m, 3H), 7.09 (d, $J = 8.2$ Hz, 1H), 6.43 (dd, $J = 16.9, 10.1$ Hz, 1H), 6.26 (dd, $J = 16.9, 2.0$ Hz, 1H), 5.77 (dd, $J = 10.1, 2.0$ Hz, 1H), 3.63 (t, $J = 4.3$ Hz, 4H), 3.07 (s, 2H), 2.53–2.48 (m, 4H); ^{13}C NMR (DMSO- d_6): δ 167.9, 165.2, 164.1, 163.8, 158.1, 152.7, 140.8, 137.4, 136.8, 132.7, 132.1, 130.4, 127.8, 123.7, 120.3 (2C), 119.3 (2C), 117.6, 117.0, 113.2, 108.0, 66.6 (2C), 62.5, 53.7 (2C); HRMS (ESI) for $C_{27}H_{25}N_5O_5S$, $[M+H]^+$ calcd: 553.1628, found: 553.1641.

4.2.11. *N*-(3-(2-(4-((1-morpholino)acetyl)amino)-3-chlorophenylamino)thieno[3,2-*d*]pyrimidin-4-yloxy)phenyl)acrylamide (**9k**)

Yield 12.6%; off-gray solid. 1H NMR (DMSO- d_6): δ 10.37 (s, 1H), 9.71 (s, 1H), 9.65 (s, 1H), 8.34 (d, $J = 5.4$ Hz, 1H), 7.89 (d, $J = 9.0$ Hz, 1H), 7.86 (s, 1H), 7.79 (t, $J = 2.2$ Hz, 1H), 7.59 (dd, $J = 8.1, 2.2$ Hz, 1H),

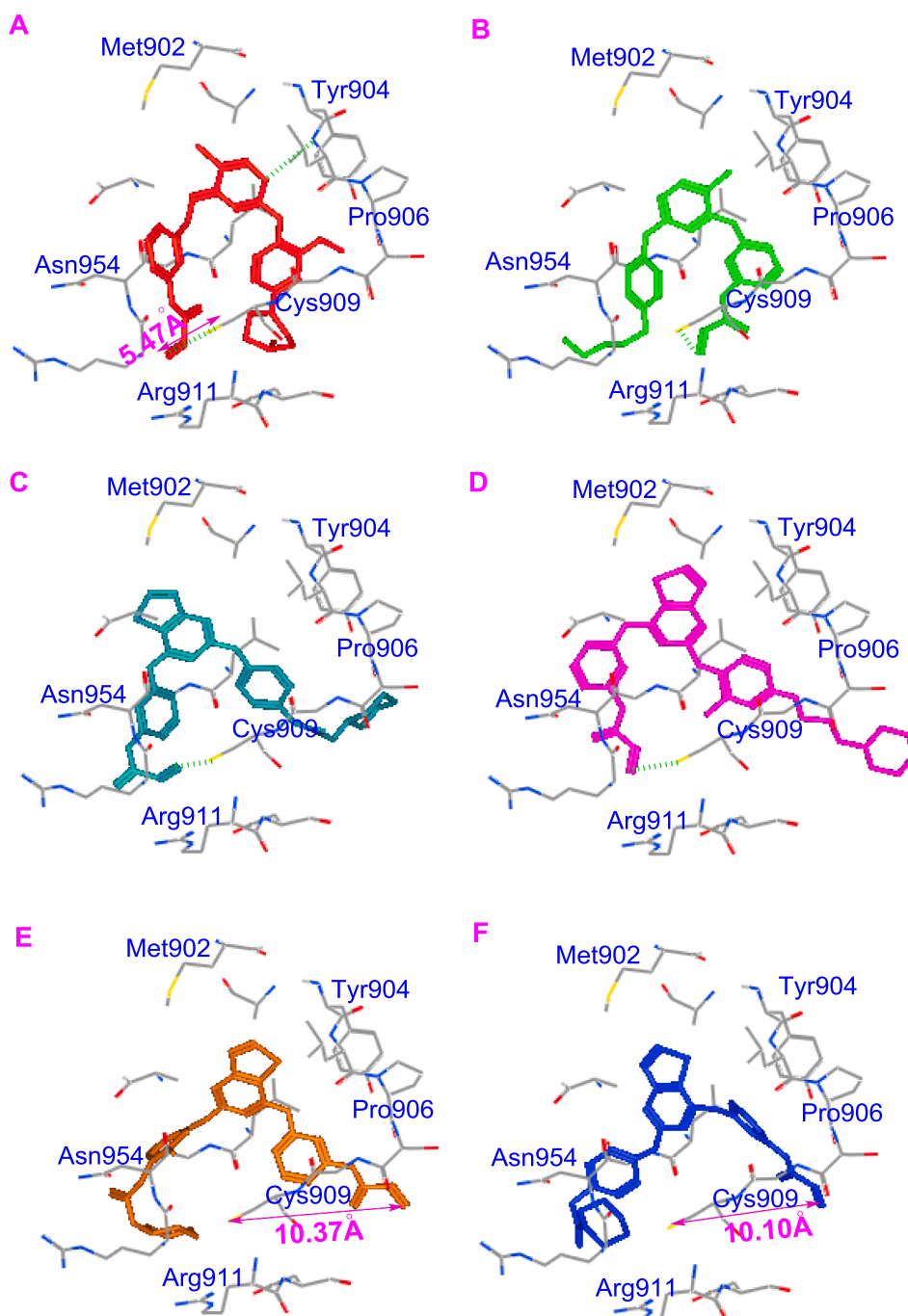


Fig. 10. Proposed binding models of the typical inhibitors with JAK3 (PDB code:4Z16), A: **8**, B: Spebrutinib, C: inhibitor **9g**, D: inhibitor **9a**, E: inhibitor **9k**, F: inhibitor **9i**.

7.53–7.44 (m, 2H), 7.41 (d, $J = 5.4$ Hz, 1H), 7.10 (dd, $J = 8.1, 2.2$ Hz, 1H), 6.43 (dd, $J = 16.8, 10.0$ Hz, 1H), 6.25 (dd, $J = 16.8, 2.0$ Hz, 1H), 5.77 (dd, $J = 10.0, 2.0$ Hz, 1H), 3.67 (t, $J = 4.6$ Hz, 4H), 3.14 (s, 2H), 2.60–2.53 (m, 4H); ^{13}C NMR (DMSO- d_6): δ 168.2, 165.0, 164.2, 163.8, 157.8, 152.6, 141.0, 138.2, 137.8, 132.1, 130.5, 128.2, 127.8, 124.1, 123.7, 122.6, 118.7, 118.0, 117.4, 117.3, 113.1, 108.6, 66.9 (2C), 62.0, 53.6 (2C); HRMS (ESI) for $\text{C}_{27}\text{H}_{25}\text{ClN}_6\text{O}_4\text{S}$, $[\text{M} + \text{H}]^+$ calcd: 565.1419, found: 565.1410.

4.3. Kinase enzymatic assays

All the enzymatic assays were tested applying with the ADP-Glo™ assay system (BTK: Catalog. V2941, JAK3: Catalog. V3701), were

purchased from Promega Corporation (USA). The experiments were performed according to the instructions of the manufacturer. The detailed and complete protocols, and the active kinase data were available at: <https://cn.promega.com/products/cell-signaling/kinase-assays-and-kinase-biology/btk-kinase-enzyme-system/?catNum=V2941> and <https://cn.promega.com/products/cell-signaling/kinase-assays-and-kinase-biology/jak3-kinase-enzyme-system/?catNum=V3701>, respectively. For all of the tested compounds, concentrations consisting of suitable levels from 0.1 to 1000 nM were used. The test was performed in a 384-well plates, including the main steps below: 1) perform a 5 μL kinase reaction using $1 \times$ kinase buffer (e.g., $1 \times$ reaction buffer A), 2) incubate at room temperature for 60 min, 3) add 5 μL of ADP-Glo™ reagent to stop the kinase reaction and deplete the unconsumed ATP,

leaving only ADP and a very low background of ATP, 4) incubate at room temperature for 40 min, 5) add 10 μL of kinase detection, 6) reagent to convert ADP to ATP and introduce luciferase and Luciferin to detect ATP, 7) incubate at room temperature for 30 min, 8) plates was measured on TriStar® LB942 Multimode MicroplateReader (BERTHOLD) to detect the luminescence (Integration time 0.5–1 s). Curve fitting and data presentations were performed using GraphPad Prism version 8.0.

4.4. Cells and reagents

Ramos, Raji, Namalwa and L-02 cells were purchased from Fuheng Biology Company (Shanghai, China). Peripheral blood mononuclear cells (PBMC) were obtained from a healthy adult male. The Cell Counting Kit-8 (CCK-8) reagent was purchased from Biotool Company (Switzerland). The BTK enzyme and the ADP-Glo™ Kinase Assay system that measures ADP formed from a kinase reaction were purchased from Promega Corporation (USA).

4.5. Cellular activity assay

Ramos, Raji, Namalwa cells viability assays were performed according to the CCK-8 method. The cells were seeded in 96-well plates at a density of 3000, 8000, 7000 cells/well and were maintained at 37 °C in a 5% CO₂ incubator in RPMI-1640 containing 10% fetal bovine serum (FBS, Gibco) for 4 h. Cells were exposed to treatment for 72 h, and the number of cells used per experiment for each cell lines was adjusted to obtain an absorbance of 0.5–1.2 at 450 nm with a microplate reader (Thermo Fisher, USA). Compounds were tested at appropriate concentrations (1.25–40 μM), with each concentration duplicated five times. The IC₅₀ values were calculated using GraphPad Prism version 8.0.

4.6. AO/EB staining assay

Approximately 2×10^5 cells/well of Ramos and Raji cells in 6-well plates were incubated in an incubator for 48 h, then treated with different concentrations of inhibitors for 48 h. Then, total of 20 μL of the solution containing the AO/EB dye mix (1.0 $\mu\text{g}/\text{mL}$ of AO and 1.0 $\mu\text{g}/\text{mL}$ of EB in PBS) was added to the cells. The apoptotic, necrotic, and live cells were observed under the fluorescent microscope (OLYMPUS, Tokyo, Japan).

4.7. Cytotoxic activity assay

Peripheral venous blood was collected in an ACD anticoagulant (V_{blood}: V_{anticoagulant} = 9:1) tube from the normal healthy adult male. The leucocyte-rich plasma was removed and the peripheral blood mononuclear cells (PBMC) consisting of monocytes and the lymphocytes were separated on Lymphoprep (density 1.077 g/mL, Nyegaard & Co. As., Oslo, Norway). The cells collected from the interface layer were washed three times with PBS buffered salt solution and counted using cell counting chamber.

PBMC cells were seeded in 24-well plates at a density of 200,000 to 250,000 cells/well. Cells were treated with inhibitors **9a** at appropriate concentration (5, 10, 20 μM), with each concentration duplicated five times. After maintaining the cells at 37 °C, in a 5% CO₂ incubator in RPMI-1640 containing 10% fetal bovineserum (FBS, Gibco) for 24 h, the morphology of the cells was observed with a phase contrast microscope (Nikon, Japan), and the number of living PBMC cells was calculated by traditional manual method with an ordinary cell counting chamber.

4.8. Flow cytometry assay

The Ramos cells (2×10^5 cells/well) incubated in 6-well plates were treated with solvent control (DMSO), Spebrutinib or **9a** in

medium containing 5% FBS for 48 h. Then, collected and fixed with 70% ethanol at 4 °C overnight. After being fixed with 70% ethanol at 4 °C, the cells were stained with Annexin V-FITC (5 μL)/propidium iodide (5 μL), and analyzed by flow cytometry assay (Becton-Dickinson, USA). For cell cycle analysis, Ramos cells at a density of approximately 2×10^5 cells/well were incubated in 6-well plates, treated with different concentrations of inhibitors for 48 h, collected and fixed with 70% ethanol at 4 °C overnight. After fixation, the cells were washed with PBS and stained with propidium iodide (PI) for 30 min under subdued light. Stained cells were analyzed flow cytometry assay (Becton-Dickinson, USA).

4.9. Western blotting assay

The lysates from Namalwa cells in different groups were extracted and centrifuged at 14,000g for 15 min at 4 °C, then the total proteins were obtained. An aliquot (40 μg protein) was loaded onto a 8–12% SDS-PAGE gels and separated electrophoretically. Then the target proteins were transferred to a PVDF membrane (Millipore, USA). After blocking the PVDF membrane in 5% dried skim milk (Boster Biological Technology, China) for 2 h at room temperature, the membrane was incubated overnight at 4 °C with primary antibodies for 12 h. Protein detection was performed based on an enhanced chemiluminescence (ECL) method and photographed by using a BioSpectrum Gel Imaging System (HR410, UVP, USA). In order to eliminate the variations, data were adjusted to β -Actin expression: IOD of objective protein versus IOD of β -Actin expression.

4.10. Molecular docking study

The AutoDock 4.2 software was used to perform the docking exploration. Detailed tutorials that guide users through basic AutoDock usage, docking with flexible rings, and virtual screening with AutoDock may be found at: <http://autodock.scripps.edu/faqs-help/tutorial>. Generally, the crystal structure (PDB: 4Z16) of the kinase domain of JAK3 bound to inhibitor **9a** was used in the docking studies. The enzyme preparation and the hydrogen atoms adding was performed in the prepared process. The whole JAK3 enzyme was defined as a receptor and the site sphere was selected on the basis of the binding location of Spebrutinib. By moving Spebrutinib and the irrelevant water, molecule **9a**. The binding interaction energy was calculated to include Van der Waals, electrostatic, and torsional energy terms defined in the TRIPOS force field. The structure optimization was performed using a genetic algorithm, and only the best-scoring ligand protein complexes were kept for analyses.

4.11. Statistical analysis

All data were displayed as a mean \pm SD. The statistical difference between two groups was tested by ANOVA test and Tukey's multiple comparison test. $p < 0.05$ was considered statistically significant.

Declaration of Competing Interest

We want to submit the revised manuscript in the category of research articles titled “JAK3 inhibitors based on thieno[3,2-*d*]pyrimidine scaffold: design, synthesis and bioactivity evaluation for the treatment of B-cell lymphoma”. There are no concerns about third-party copyright or conflicts of interest or online supplementary material.

Acknowledgements

We are grateful to the National Natural Science Foundation of China (No. 81672945), the “Xing Liao” Talents Project of Liaoning province, China (XLYC1807011), the Research Fund of Higher Education of Liaoning province (LZ2019004), the Natural Science Foundation of

Liaoning province (20180530066), the Cultivation Project of Youth Tech stars, Dalian, China (No. 2016RQ043), and the Foundation of Science and Technology Innovation of Dalian, China (2019J13SN76) for the financial support of this research.

References

- [1] A.J. Steele, A.G. Prentice, K. Cwynarski, A.V. Hoffbrand, S.M. Hart, M.W. Lowdell, E.R. Samuel, R.G. Wickremasinghe, The JAK3-selective inhibitor PF-956980 reverses the resistance to cytotoxic agents induced by interleukin-4 treatment of chronic lymphocytic leukemia cells: potential for reversal of cytoprotection by the microenvironment, *Blood* 116 (2010) 4569–4577.
- [2] J. Nakayama, M. Yamamoto, K. Hayashi, H. Satoh, K. Bundo, M. Kubo, R. Goitsuka, M.A. Farrar, D. Kitamura, BLNK suppresses pre-B-cell leukemogenesis through inhibition of JAK3, *Blood* 113 (2009) 1483–1492.
- [3] E.A. Sudbeck, X.P. Liu, R.K. Narla, S. Mahajan, S. Ghosh, C. Mao, F.M. Uckun, Structure-based design of specific inhibitors of Janus kinase 3 as apoptosis-inducing antileukemic agents, *Clin. Cancer Res.* 5 (1999) 1569–1582.
- [4] W. Damsky, B.A. King, JAK inhibitors in dermatology: The promise of a new drug class, *J. Am. Acad. Dermatol.* 76 (2017) 736–744.
- [5] K. Yamaoka, P. Saharinen, M. Pesu, V.E. Holt, O. Silvennoinen, J.J. O'Shea, The Janus kinases (Jaks), *Genome Biol.* 5 (2004) 253.
- [6] J.W. Verbsky, E.A. Bach, Y.F. Fang, L. Yang, D.A. Randolph, L.E. Fields, Expression of Janus kinase 3 in human endothelial and other non-lymphoid and non-myeloid cells, *J. Biol. Chem.* 271 (1996) 13976–13980.
- [7] J. Mishra, C.M. Waters, N. Kumar, Molecular mechanism of interleukin-2-induced mucosal homeostasis, *Am. J. Physiol. Cell. Physiol.* 302 (2012) C735–C747.
- [8] M.B. Marrero, B. Schieffer, W.G. Paxton, L. Heerd, B.C. Berk, P. Delafontaine, K.E. Bernstein, Direct stimulation of Jak/STAT pathway by the angiotensin II AT1 receptor, *Nature* 375 (1995) 247–250.
- [9] W. Wu, X. Sun, Janus kinase 3: the controller and the controlled, *Acta Biochim. Biophys. Sin. (Shanghai)* 44 (2012) 187–196.
- [10] K. West, CP-690550, a JAK3 inhibitor as an immunosuppressant for the treatment of rheumatoid arthritis, transplant rejection, psoriasis and other immune-mediated disorders, *Curr. Opin. Investig. Drugs.* 10 (2009) 491–504.
- [11] C. Harrison, J.J. Kiladjian, H.K. Al-Ali, H. Gisslinger, R. Waltzman, V. Stalbovskaya, M. McQuitty, D.S. Hunter, R. Levy, F. Cervantes, A.M. Vannucchi, T. Barbui, G. Barosi, JAK inhibition with ruxolitinib versus best available therapy for myelofibrosis, *N. Engl. J. Med.* 366 (2012) 787–798.
- [12] K.V. Jensen, O. Cseh, A. Aman, S. Weiss, H.A. Luchman, The JAK2/STAT3 inhibitor pacritinib effectively inhibits patient-derived GBM brain tumor initiating cells in vitro and when used in combination with temozolomide increases survival in an orthotopic xenograft model, *PLoS One* 12 (2017) e0189670.
- [13] K.A. Monaghan, T. Khong, C.J. Burns, A. Spencer, The novel JAK inhibitor CYT387 suppresses multiple signalling pathways, prevents proliferation and induces apoptosis in phenotypically diverse myeloma cells, *Leukemia* 25 (2011) 1891–1899.
- [14] Z. Lu, C.C. Hong, P.C. Jark, A.L.F.V. Assumpção, N. Bollig, G. Kong, X. Pan, JAK1/2 Inhibitors AZD1480 and CYT387 Inhibit Canine B-Cell Lymphoma Growth by Increasing Apoptosis and Disrupting Cell Proliferation, *J. Vet. Intern. Med.* 31 (2017) 1804–1815.
- [15] S. Hart, K.C. Goh, V. Novotny-Diermayr, Y.C. Tan, B. Madan, C. Amalini, L.C. Ong, B. Kheng, A. Cheong, J. Zhou, W.J. Chng, J.M. Wood, Pacritinib (SB1518), a JAK2/FLT3 inhibitor for the treatment of acute myeloid leukemia, *Blood Cancer J.* 1 (2011) e44.
- [16] M. Cetkovic-Cvrlje, A.L. Dragt, A. Vassilev, X. Liu, F.M. Uckun, Targeting JAK3 with JANEX-1 for prevention of autoimmune type 1 diabetes in NOD mice, *Clin. Immunol.* 106 (2003) 213–225.
- [17] S. Barua, J.I. Chung, A.Y. Kim, S.Y. Lee, S.H. Lee, E.J. Baik, Jak kinase 3 signaling in microgliogenesis from the spinal nestin+ progenitors in both development and response to injury, *Neuroreport* 28 (2017) 929–935.
- [18] Q. Liu, Y. Sabnis, Z. Zhao, T. Zhang, S.J. Buhrlage, L.H. Jones, N.S. Gray, Developing irreversible inhibitors of the protein kinase cysteinome, *Chem. Biol.* 20 (2013) 146–159.
- [19] A. Thorarensen, M.E. Dowty, M.E. Banker, B. Juba, J. Jussif, T. Lin, F. Vincent, R.M. Czerwinski, A. Casimiro-Garcia, R. Unwalla, J.I. Trujillo, S. Liang, P. Balbo, Y. Che, A.M. Gilbert, M.F. Brown, M. Hayward, J. Montgomery, L. Leung, X. Yang, S. Soucy, M. Hegen, J. Coe, J. Langille, F. Vajdos, J. Chrencik, J.B. Telliez, Design of a Janus kinase 3 (JAK3) Specific Inhibitor 1-((2S,5R)-5-((7H-Pyrrolo[2,3-d]pyrimidin-4-yl)amino)-2-methylpiperidin-1-yl)prop-2-en-1-one (PF-06651600) Allowing for the Interrogation of JAK3 signaling in Humans, *J. Med. Chem.* 60 (2017) 1971–1993.
- [20] J. Kempson, D. Ovalle, J. Guo, S.T. Wroblewski, S. Lin, S.H. Spergel, J.J. Duan, B. Jiang, Z. Lu, J. Das, B.V. Yang, J. Hynes Jr., H. Wu, J. Tokarski, J.S. Sack, J. Khan, G. Schieven, Y. Blatt, C. Chaudhry, L.M. Salter-Cid, A. Fura, J.C. Barrish, P.H. Carter, W.J. Pitts, Discovery of highly potent, selective, covalent inhibitors of JAK3, *Bioorg. Med. Chem. Lett.* 27 (2017) 4622–4625.
- [21] L. Tan, K. Akahane, R. McNally, K.M. Reyskens, S.B. Ficarro, S. Liu, G.S. Herter-Sprie, S. Koyama, M.J. Pattison, K. Labella, L. Johannessen, E.A. Akbay, K.K. Wong, D.A. Frank, J.A. Marto, T.A. Look, J.S. Arthur, M.J. Eck, N.S. Gray, Development of selective covalent janus kinase 3 inhibitors, *J. Med. Chem.* 58 (2015) 6589–6606.
- [22] D. Zhao, S. Huang, M. Qu, C. Wang, Z. Liu, Z. Li, J. Peng, K. Liu, Y. Li, X. Ma, X. Shu, Structural optimization of diphenylpyrimidine derivatives (DPPYs) as potent Bruton's tyrosine kinase improved activity toward B leukemia cell lines, *Eur. J. Med. Chem.* 126 (2017) 444–455.
- [23] Y. Ge, Y. Jin, C. Wang, J. Zhang, Z. Tang, J. Peng, K. Liu, Y. Li, Y. Zhou, X. Ma, Discovery of novel Bruton's tyrosine kinase (BTK) inhibitors bearing a N,9-diphenyl-9H-purin-2-amine scaffold, *ACS Med. Chem. Lett.* 7 (2016) 1050–1055.
- [24] Y. Ge, H. Yang, C. Wang, Q. Meng, L. Li, H. Sun, Y. Zhen, K. Liu, Y. Li, X. Ma, Design and synthesis of phosphoryl-substituted diphenylpyrimidines (Pho-DPPYs) as potent Bruton's tyrosine kinase (BTK) inhibitors: Targeted treatment of B lymphoblastic leukemia cell lines, *Bioorg. Med. Chem.* 25 (2017) 765–772.
- [25] A. Song, J. Zhang, Y. Ge, C. Wang, Q. Meng, Z. Tang, J. Peng, K. Liu, Y. Li, X. Ma, C-2 (E)-4-(Styryl)aniline substituted diphenylpyrimidine derivatives (Sty-DPPYs) as specific kinase inhibitors targeting clinical resistance related EG^{FR1790M} mutant, *Bioorg. Med. Chem.* 25 (2017) 2724–2729.
- [26] Z. Song, S. Huang, H. Yu, Y. Jiang, C. Wang, Q. Meng, X. Shu, H. Sun, K. Liu, Y. Li, X. Ma, Synthesis and biological evaluation of morpholine-substituted diphenylpyrimidine derivatives (Mor-DPPYs) as potent EG^{FR1790M} inhibitors with improved activity toward the gefitinib-resistant non-small cell Lung cancers (NSCLC), *Eur. J. Med. Chem.* 133 (2017) 329–339.